# Structure-Based Virtual Screening for the Discovery of Natural Inhibitors for Human Rhinovirus Coat Protein

Judith M. Rollinger,*,† Theodora M. Steindl,‡ Daniela Schuster,‡ Johannes Kirchmair,‡ Kathrin Anrain,† Ernst P. Ellmerer,§ Thierry Langer,‡ Hermann Stuppner,† Peter Wutzler,|| and Michaela Schmidtke||

*Institute of Pharmacy/Pharmacognosy and Center for Molecular Biosciences Innsbruck, Institute of Pharmacy/Pharmaceutical Chemistry and Center for Molecular Biosciences Innsbruck, and Institute of Organic Chemistry and Center for Molecular Biosciences Innsbruck, University of Innsbruck, Innrain 52, A-6020 Innsbruck, Austria, and Institute of Virology and Antiviral Therapy, Friedrich Schiller University, Hans-Knoell-Straße 2, D-07745 Jena, Germany*

*Received June 26, 2007*

Inhibitors of the human rhinovirus (HRV) coat protein are promising candidates to treat and prevent a number of upper respiratory diseases. The aim of this study was to find antiviral compounds from nature, focusing on the HRV coat protein. Through computational structure-based screening of an in-house 3D database containing 9676 individual plant metabolites from ancient herbal medicines, combined with knowledge from traditional use, we selected sesquiterpene coumarins from the gum resin asafetida as promising natural products. Chromatographic separation steps resulted in the isolation of microlobidene (**1**), farnesiferol C (**2**), farnesiferol B (**3**), and kellerin (**4**). Determination of the inhibition of the HRV-induced cytopathic effect for serotypes 1A, 2, 14, and 16 revealed a dose-dependent and selective antirhinoviral activity against serotype 2 for asafetida ($IC_{50}$ = 11.0 $\mu$g/mL) and its virtually predicted constituents **2** ($IC_{50}$ = 2.5 $\mu$M) and **3** ($IC_{50}$ = 2.6 $\mu$M). Modeling studies helped to rationalize the retrieved results.

## Introduction

Human rhinoviruses (HRV[a]) are members of the largest genus (rhinoviridae) in the picornavirus family and are comprised of over 100 different virus serotypes.[1] They are the single most important etiological agents of the common cold.[2,3] Though this upper respiratory illness is mild and self-limiting, it is of high socioeconomic impact caused by missed school or work and inappropriate therapy with antimicrobial agents.[4] Furthermore, HRV infections are associated with acute exacerbations of respiratory disease, including asthma, sinusitis, and otitis media. Results from recent studies indicate that rhinoviruses can also replicate in the lower respiratory tract and induce fever, pneumonia, and gastrointestinal symptoms.[5,6] Currently, no antiviral agents that are active against picornaviruses are available for clinical use, though extensive research efforts have led to the discovery of many potent antiviral agents. The most promising mechanisms to interfere with small chemical entities deal with virus attachment, uncoating, virus RNA replication, or viral protein synthesis and processing.[3,7] The most advanced antiviral agent in clinical trials is pleconaril, a novel viral capsid-binding inhibitor with potent and highly specific in vitro activity against the majority of serotypes of rhinoviruses and enteroviruses.[8–10] However, pleconaril is not recommended for the treatment of a cold in adults, primarily based on drug interactions,[11] marginal treatment effect,[12] and the possibility of transmission of resistant virus.[13] From this perspective, there is a high medical need to find improved antiviral agents for either the prevention or therapy of diseases caused by HRV infection.

The viral capsid, which encapsulates a single-stranded positive-sense RNA, is a promising and intensively studied target for drug development. It consists of 60 repeating protomeric units, each containing four different viral proteins (VP1–4). On the capsid surface, there is a hydrophobic pocket situated at the bottom of a depression. In the absence of an inhibitor, this so-called canyon of most rhinoviruses is occupied by a pocket factor, proposed to be a fatty acid. On the basis of the amino acid sequence identity of VP 1, the genus rhinoviruses were subdivided into two species A and B containing all but one serotype.[8] According to this classification, HRV-1A, -2, and -16 belong to the 75 serotypes of species A. HRV-B species comprises 25 serotypes, including for example HRV-3, -14, and -27. Independently from this molecular-biological classification, rhinoviruses have been grouped depending on receptor specificity and susceptibility to antiviral compounds. The majority of HRVs (major receptor group, e.g. serotypes 3, 14, 16, and 39) bind to human intercellular adhesion molecule 1 (ICAM-1),[14,15] while about ten serotypes (minor receptor group, e.g. serotypes 1A and 2) bind to various members of the low-density lipoprotein receptor. Furthermore, HRVs have been classified into antiviral groups A and B according to their sensitivity toward a panel of antiviral compounds of different length.[16] Whereas members of group B (e.g., serotypes 1A, 2, and 16) were more sensitive to short compounds,[16] longer compounds prevent replication of viruses of group A (e.g., HRV-3 and -14). Therefore, Andries and coauthors suggested that HRV members of group B must all have smaller pockets than viruses of group A.

Small antiviral compounds, such as pleconaril, may enter the HRV hydrophobic pocket and displace the existing pocket factor.[17] This results in a slight deformation of the canyon region, which affects virus replication by preventing virus attachment to cell surfaces and/or uncoating of viruses.[18] The structural organization of the viral capsid of several HRVs has

* To whom correspondence should be addressed. Phone: +43 512 507 5308. Fax: +43 512 507 2939. E-mail: judith.rollinger@uibk.ac.at.
† Institute of Pharmacy/Pharmacognosy, University of Innsbruck.
‡ Institute of Pharmacy/Pharmaceutical Chemistry, University of Innsbruck.
§ Institute of Organic Chemistry, University of Innsbruck.
|| Institute of Virology and Antiviral Therapy, Friedrich Schiller University.

[a] Abbreviations: $CC_{50}$, 50% cytotoxic concentration; CPE, cytopathic effect; 3D database, three-dimensional multiconformational database; HBA, hydrogen bond acceptor group; H, hydrophobic feature; HRV, human rhinoviruses; $IC_{50}$, 50% inhibitory concentration; SI, selectivity index; VP, viral protein.

10.1021/jm701494b CCC: $40.75 
Published on Web 02/05/2008

been elucidated by crystallization and resolution of the three-dimensional structure. They show a high structural conservation in the hydrophobic pocket among the different serotypes and, thus, permit the development of broad-spectrum anti-HRV agents.[19,20]

For the targeted selection of natural products endowed with antiviral activity, an in silico approach was performed. The potential of structure-based pharmacophore modeling as a screening tool for successful 3D database search is widely accepted in medicinal chemistry,[21] but until now it has not been widely accepted in natural product chemistry.[22]

A structure-based pharmacophore model for human rhinovirus coat protein inhibitors was generated by using the software tool Catalyst (Catalyst version 4.11). In an earlier study, this model was applied in a 3D database screening in order to validate its quality. In combination with docking and principle component analysis-based clustering methods, the model led to the successful selection of novel structures from a commercially available compound collection that showed antirhinoviral activity down to the low micromolar range.[23] After this initial proof that the pharmacophore model is able to identify active molecules from databases, it was applied for further screening operations with the aim of finding new lead structures, preferably natural products, capable of inhibiting the HRV.

For the virtual screening filtering experiments, we used our in-house 3D database DIOS.[24] The library consists of about 10 000 secondary metabolites originating from some 800 medicinal plants witnessed by Pedanius Dioscorides (1 cent. AD) in his *De materia medica*, which represents a great repository of botanical, medical, and pharmacological lore. On the basis of the in silico predictions and hints from ethnopharmacology, we focused on asafetida as the starting material to obtain the virtually predicted ligands of the HRV coat protein, belonging to the chemical class of sesquiterpene umbelliferons.

Asafetida is the commercial gum resin obtained from the roots of a variety of foul-smelling *Ferula* species (Apiaceae), particularly *F. assa-fetida* L. and *F. fetida* (BUNGE) REGEL.[25] Most of them are endemic to Eastern Iran and Western Afghanistan. In Central Asia, asafetida is a prominent culinary spice due to its offensive garliclike smell. To date, it has also been used in folk medicine for a host of indications because of its appetizing, digestive, antimicrobial, and antihelminthic properties.[26] Whereas a number of sulfides and polysulfides are responsible for the sensory properties of asafetida, the main constituents of the nonvolatile fraction belong to sesquiterpene coumarin ethers.[27,28] Some of these compounds have previously been reported to show distinct bioactivities, for example antileishmanial activity and[29] inhibition of NF-$\kappa$B,[30] of succinate ubiquinone reductase,[31] and of NO production.[32]

In our ongoing efforts to validate the potential of the computer-aided approach for the discovery of new drug leads from nature,[22,24,33,34] we scrutinized the obtained virtual hits considering pharmacological and phytochemical aspects. This prompted us to isolate some sesquiterpene umbelliferons from asafetida according to the prediction of the pharmacophore-based virtual screening and the scientifically untapped ethnopharmacological hints from the ancient sources. For biological evaluation, the antiviral activities of the gum resin and its isolated constituents were assessed by an exploratory determination of the inhibition of the cytopathic effect (CPE) induced by HRV serotypes 1A, 2, 14, and 16.

## Results and Discussion

**Pharmacophore-Based Virtual Screening.** Entries from the Protein Data Bank (PDB)[35] 1QJU and 1C8M, both complexes of HRV serotype 16 with highly active inhibitors, served as starting points for model generation.[19] The model was designed to combine features characteristic for ligand binding in the hydrophobic pocket within the HRV capsid. Four hydrophobic features (H) represent the predominately lipophilic character of the pocket realized in all known inhibitor structures. A hydrogen bond acceptor (HBA) shows another typical interaction, a direct or more often water-mediated hydrogen bond to Leu100. The features are arranged in a long stretched out fashion modeling the "tunnel"-shape of the pocket. For this closed and sterically well defined binding site, the application of a shape was useful in providing spatial limitation of the ligand size. The 3D coordinates for feature setting and the shape were derived from the PDB complex 1QJU and its bound inhibitor WIN 61209 (Chart 1). For enhanced restrictivity, another interaction possibility seen in the most well-known HRV coat protein inhibitor pleconaril (Chart 1) was realized within the model. A customized hydrogen bond acceptor containing fluorine (HBAF) to Tyr144, which is located in the very inner part of the pocket, was added using crystal structure information from PDB entry 1C8M. The resulting five-feature hypothesis is shown in Figure 1. For natural compound database screening, the HBAF feature could have been replaced by a regular HBA feature, but we preferred to keep the original model as described in the previous study unchanged.[23]

**Chart 1.** Highly Active HRV Coat Protein Inhibitors WIN 61209 (left) and Pleconaril (right)

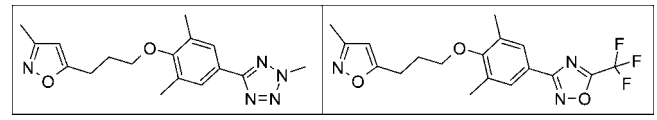

In Catalyst, the virtual screening was performed by using the best flexible search algorithm. The latter gives a certain amount of flexibility to already precalculated compound conformations when mapping them to a hypothesis and is therefore more tolerant in accepting a molecule as a hit than is the fast algorithm. This search mode is only exercisable for highly selective hypotheses, such as the model used in our study. Within the library DIOS, 0.3% or 29 compounds were returned and ranked according to their best fit values, a measurement of how well they are able to map the model features (Table 1).

The virtual screening filtering process revealed hits from various chemical classes (Table 1). About one-third of them belong to derivatives of fatty acids or alcohols showing saturated or unsaturated hydrocarbon chains with 14−20 C-atoms and an HBA group at a certain distance to the acid, ester, or alcohol group, respectively. The retrieval of these compounds is not surprising, since the binding site of the HRV canyon is frequently occupied by a fatty acid acting as a pocket factor.[19,36] A further chemical class consists of benzofuran derivatives representing constituents of the genera *Ononis* and *Medicago* (Fabaceae) or from the gum resin Styrax (*Styrax officinalis*, Styracaceae). The coumarine scaffolds among the hit list fall into two main types: (i) coumarin dimers from the medicinal plant *Ruta graveolens* (Rutaceae) and (ii) sesquiterpene coumarins from asafetida (derived from different *Ferula* species, Apiaceae). All of the putative virtual hits were prioritized with respect to their compliance with Lipinski's rule of five,[37] their pharmacological profile (as far as known from literature), their content in the plant matrix, and the accessibility of the plants.

For the final selection of plant material used for phytochemical investigations and isolation of virtual hits, the ethnopharmacological use described by Dioscorides was consulted. As

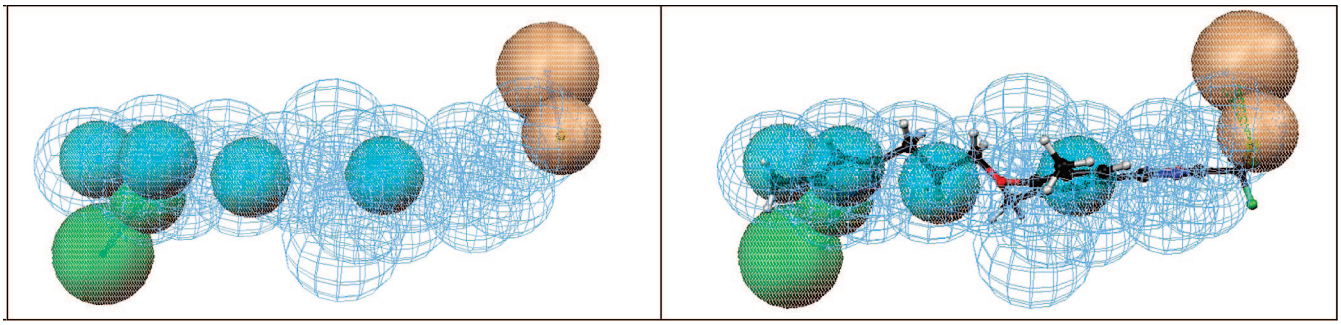

**Figure 1.** Structure-based pharmacophore hypothesis for HRV coat protein inhibitors built within the program Catalyst: hypothesis alone (left) and pleconaril mapped onto hypothesis (right). Pharmacophore features are color-coded: HBA (green), HBAF (customized function) (orange), H (cyan), and shape (blue).

shown in a previous study, the probability of discovering real hits from in silico predictions can be increased significantly by considering hints from folk medicine.[24] Among the aforementioned medicinal plants, only asafetida is reported to be effective in the context of upper respiratory diseases. On the basis of the descriptions given in the *De materia medica*, there is strong evidence that the "juice" (i.e., resin) of the popular ancient *silphion* originating from Media and Syria corresponds to asafetida (book III, cap. 80).[38] Yielded by incision of the root and stalk and frequently mixed with *sagapenon*, that is, the resin of *F. persica* Willd. (book III, cap. 81),[38] asafetida is reported to be effective "for chronic harshness of the throat"; "it clears the voice" and "shrinks the uvulas"; it is "suitable for a cough", "for pleurisy", and "for chest pain". *Sagapenon* is said to "clear thick matters from the lungs" and to be "given to those who are chilled".[38]

Sesquiterpene umbelliferons from asafetida were accordingly assessed as one of the most promising class of hit compounds.

**Phytochemistry.** The dichlorormethane-soluble part of asafetida was subjected to liquid/liquid partition. By using HPLC/UV/MS analysis, sesquiterpene coumarins were identified in the petrol ether fraction. Separation of the focused plant constituents was achieved by means of silica gel and sephadex column chromatography. Four sesquiterpene coumarin ethers (**1**–**4**, Chart 2) were isolated and identified by 1D- and 2D-NMR experiments, MS-analysis, optical rotation, and comparison with literature data.

The constitution of **1** deduced from 1D- and 2D-NMR spectra and comparison with the $^1$H NMR data published by Nabiev and Malikov suggested the identity of compound **1** with microlobidene isolated from *Ferula microloba* BOISS.[39] The constitution and the configuration, except the position of the OH-group (C-3′) and the orientation of the H-atom at position C-10′, were confirmed by partial synthesis starting from galbanic acid (Chart 2, **5**). The results of our 1D-NOESY experiments allowed us to assign the relative configuration at the position of the OH-group and therefore to complete the configurational assignment. Thus, the absolute configuration of microlobidene (**1**) was determined with respect to galbanic acid (**5**). A complete list of NMR resonances and the NOESY-correlations for microlobidene are given in the Supporting Information.

The structures of compounds **2** and **3** could be assigned to farnesiferols C and B, respectively, which are known as main constituents from *F. assafetida*.[40,41] The constitution of **4** was deduced from its 1D- and 2D-NMR spectra. $^1$H NMR data of this compound (labeled as kellerin) have been published by Perel'son et al.[42] and are consistent with ours. Furthermore, the relative configuration could be proven by a series of 1D-NOESY experiments. This is provided in the Supporting Information together with the summarized $^1$H and $^{13}$C NMR data. To date, kellerin has never been isolated from the gum resin asafetida or from *F. assa-fetida* and *F. fetida*, respectively, but from *F. kelleri* and *F. kokanica*.[43,44] Thus, it remains unclear whether the latter two *Ferula* species are also present in the commercial asafetida used for this study or whether kellerin is a newly detected sesquiterpene coumarin from the commonly used species *F. assa-fetida* or *F. fetida*.

Two of the isolated coumarins, namely compounds **2** (farnesiferol C, CAS 512-17-4) and **3** (farnesiferol B, CAS 54990-68-0) are among the virtual hits (Table 1). **1** and **4** however could not map all the set features of the pharmacophore model. Asafetida and all of its isolated sesquiterpene coumarins (**1**–**4**) were tested for their antiviral activity to check their correlation with the in silico predictions.

**Cytotoxicity and Antiviral Activity.** To exclude unspecific compound actions, the cytotoxicity of asafetida and its isolates was determined in HeLa cells. The 50% cytotoxic concentration ($CC_{50}$) was calculated from the mean dose–response curve of two independent assays with gum resin asafetida and its isolated constituents (**1**–**4**). The results are summarized in Table 2.

The gum resin asafetida as well as the thereof isolated sesquiterpene umbelliferons (**1**−**4**) was subjected to CPE-inhibitory assays. They were performed with pleconaril-sensitive HRV-1A, -2, -14, and -16 in HeLa cells.[8,45] The results from the CPE-inhibitory assays proved dose-dependent antiviral activities against HRV-2 for the gum resin asafetida (Table 2 and Figure 2) and for **2** and **3** (Table 2 and Figure 3). The 50% inhibitory concentrations of **2** and **3** are 2.51 and 2.61 $\mu$M, respectively. None of the tested compounds inhibited the replication of HRV-1A, -14, and -16 in HeLa cells (results not shown). The selected test viruses differ in amino acid sequence identity in VP1.[8] The highly identical HRV-1A and -16 as well as HRV-2 belong to HRV species A and HRV-14 belongs to species B. Moreover, according to Andries and coauthors, the size of the hydrophobic pocket of HRV-1A, -2, and -16 is smaller than that of HRV-14.[46]

Previously, capsid-binding compounds were shown to inactivate viruses directly or to inhibit adsorption and/or uncoating of rhinoviruses.[47–49] To evaluate the mode of action, modified plaque-reduction assays were performed with HRV-2 and compound **2** in HeLa cells. Pleconaril was included as the positive control in these studies. Direct inactivation of HRV-2 was studied by incubation of the virus with or without compound **2** at 37 °C for 1 h. Thereafter, virus suspensions were diluted 100-fold, resulting in drug concentrations below the 50% inhibitory dose. The residual titer was determined by plaque assays on HeLa cells. Whereas pleconaril inactivated HRV-2 directly, compound **2** did not (Table 3). To investigate the

**Table 1.** Chemical Structures and Best Fit Values of Those Natural Products Retrieved as Virtual Hits from the DIOS Database

| CAS-No<br>Best fit | Chemical structure | CAS-No<br>Best fit | Chemical structure |
|---|---|---|---|
| 52766-70-8<br>Best fit: 4.2 | 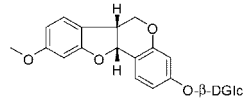 | 6799-85-5<br>Best fit: 1.9 | 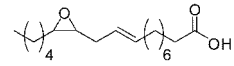 |
| 62643-46-3<br>Best fit: 3.3 | 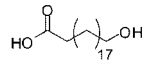 | 35121-78-9<br>Best fit: 1.8 | 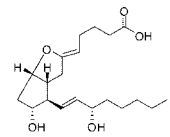 |
| 198898-36-1<br>Best fit: 3.2 | 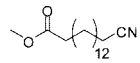 | 22474-42-6<br>Best fit: 1.7 | 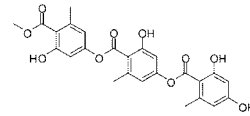 |
| 506-13-8<br>Best fit: 2.9 | 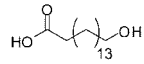 | 512-17-4<br>Best fit: 1.6 | 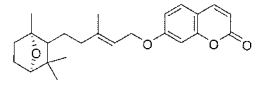 |
| 2034-69-7<br>Best fit: 2.9 | 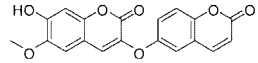 | 19812-64-7<br>Best fit: 1.4 | 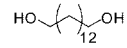 |
| 67008-88-2<br>Best fit: 2.9 | 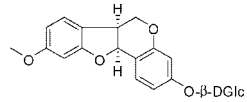 | 320624-68-8<br>Best fit: 1.4 | 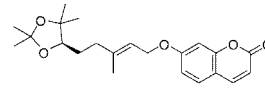 |
| 42830-33-1<br>Best fit: 2.8 | 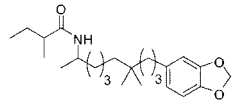 | 41015-43-4<br>Best fit: 1.3 | 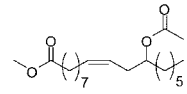 |
| 5892-54-6<br>Best fit: 2.6 | 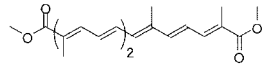 | 31328-13-9<br>Best fit: 1.3 | 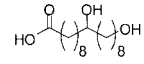 |
| 115361-83-6<br>Best fit: 2.5 | 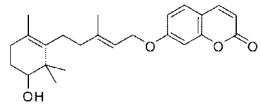 | 80931-31-3<br>Best fit: 1.3 | 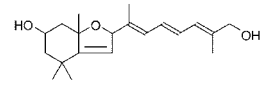 |
| 70360-15-5<br>Best fit: 2.5 | 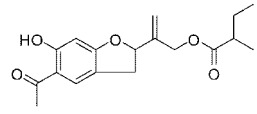 | 161928-85-4<br>Best fit: 1.1 | 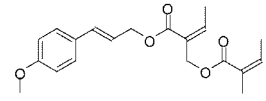 |
| 263026-24-0<br>Best fit: 2.4 | 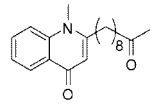 | 17375-66-5<br>Best fit: 1.0 | 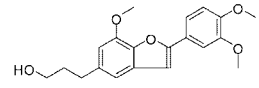 |
| 17375-67-6<br>Best fit: 2.3 | 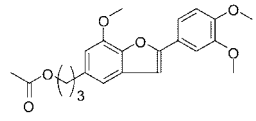 | 122617-02-1<br>Best fit: 1.0 | 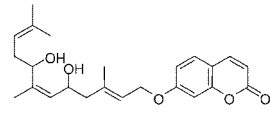 |
| 54990-68-0<br>Best fit: 2.3 | 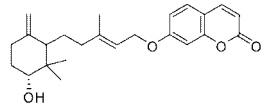 | 70615-03-1<br>Best fit: 0.5 | 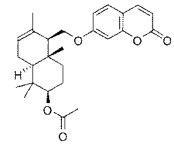 |
| 54352-98-6<br>Best fit: 2.1 | 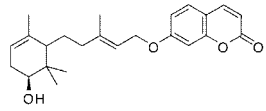 | 54397-83-0<br>Best fit: 0.4 | 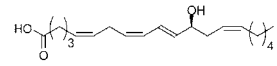 |
| 3749-38-0<br>Best fit: 1.9 | 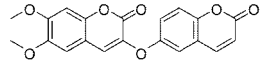 | | |

**Chart 2.** Chemical Structures of Sesquiterpene Coumarin Ethers Microlobidene (**1**), Farnesiferol C (**2**), Farnesiferol B (**3**), Kellerin (**4**), and Galbanic Acid (**5**)

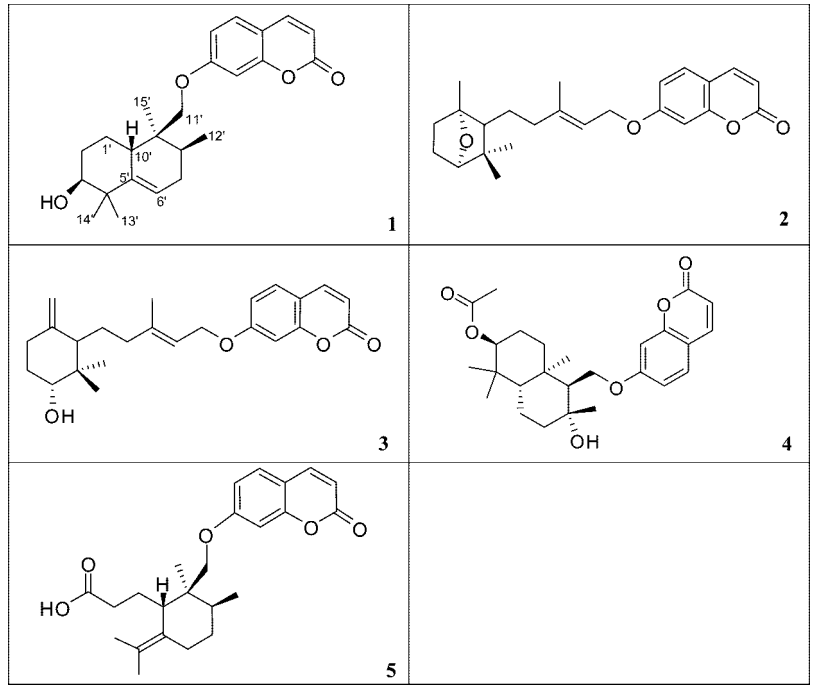


**Table 2.** Cytotoxicity and Anti-HRV-2 Activity of Gum Resin Asafetida and Compounds **1**−**4**

| sample | $CC_{50}$ (μg/mL) | $IC_{50}$ (μg/mL) | selectivity index ($CC_{50}/IC_{50}$) |
|---|---|---|---|
| pleconaril | 12.6[a] | 0.01 | 1260 |
| asafetida | 69.3 | 10.98 | 6.31 |
| **1** | 10.0 | >10.0 | <1 |
| **2** | 7.7 | 0.96 | 8.02 |
| **3** | 8.2 | 1.00 | 8.20 |
| **4** | 15.5 | >15.5 | <1 |

[a] Published previously.[45]

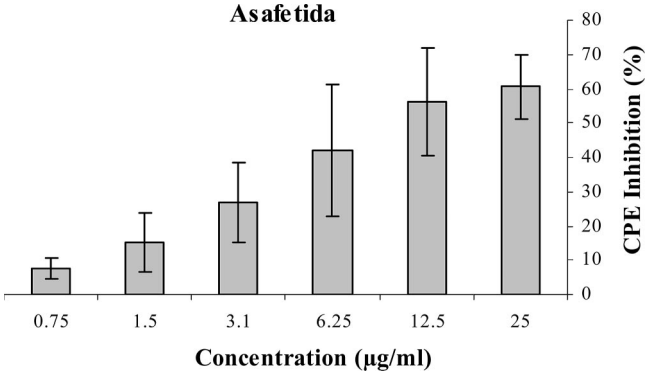


**Figure 2.** Dose-dependent inhibition of the HRV-2-induced CPE (%) in HeLa cells by asafetida. Data are means ± SD ($n = 6$).

compound effect on viral adsorption, compound **2** was added immediately before virus inoculation to the cells. Treatment was carried out during viral adsorption for 2 h at 4 °C, at which temperature the virus is prevented from entering the cells. After the adsorption period, free viruses and compound **2** were removed. When given during virus adsorption, pleconaril as well as compound **2** reduced the number of HRV-2-induced plaques, albeit at different percentages (Table 3).

**Insight into Ligand−Target Interactions. Docking.** The possible binding modes of the two active compounds **2** and **3** to the hydrophobic pocket within the HRV capsid were investigated by docking experiments. LigandFit was applied to combine classical docking with the pharmacophore concept, that is, with knowledge of favorable interaction possibilities within the binding site because it allows the definition of interaction filters. Hydrogen bonds to Leu100 and Tyr144 were selected as well as several hydrophobic amino acid parts representing regions for nonpolar interactions within the HRV coat protein site (Tyr144, Leu100, Ile122, Ile236, Tyr190, and Leu184). This can be seen as the counterpart to an eight-feature pharmacophore (two hydrogen bonds and six hydrophobic features). Both farnesiferol C (**2**) and B (**3**) got top ranks mapping seven of the defined interaction possibilities. Visual inspection also confirmed their highly favorable positioning within the binding site. Due to a second cyclization in the terpenoid moiety of compounds **1** and **4** (see Chart 2), these two natural products however were not able to fulfill the mandatory occupation in space with respect to the longitudinal orientation of the binding pocket in the hydrophobic canyon.

In order to be able to analyze more easily how well the docked molecules and poses fit into the binding pocket and make interactions with the surrounding amino acids, they were visualized within the software LigandScout.[50] The latter is a tool for automatic pharmacophore recognition, searching for interaction possibilities between a protein and a ligand in the binding site. Examples of poses and corresponding pharmacophores of farnesiferol B (**3**) can be seen in Figure 4. Although hydrogen bonds are also detected, the hydrophobic contacts are the dominating features. Obviously the ligand is able to match the highly lipophilic character of this pocket very well. This domination of hydrophobicity also provokes the 180° positional rotation of docking poses seen in all docked ligands. This phenomenon has been observed in reality in the crystal structures of two highly similar HRV coat protein inhibitors.[51] An image of the mapping of compound **3** to the site within LigandFit, which was originally defined from pleconaril, is shown in Figure 5.

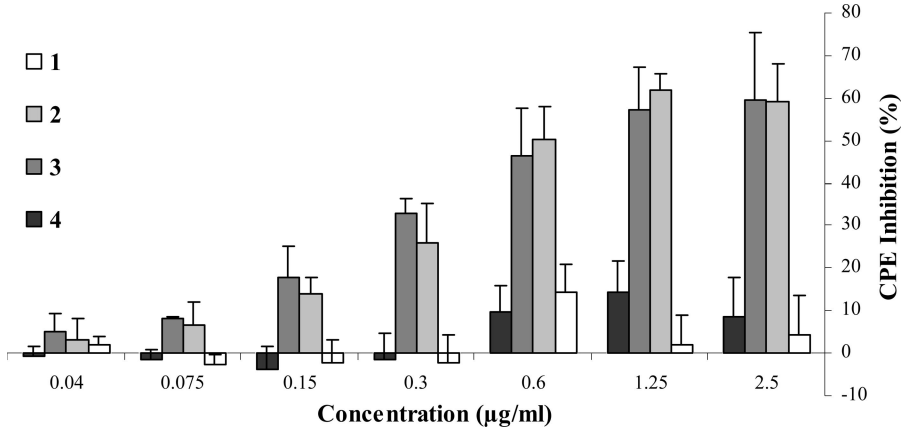


**Figure 3.** Concentration-dependent inhibition of the HRV-2 induced CPE (%) by compounds **1–4** isolated from asafetida determined in HeLa cells. Data are means ± SD ($n = 4$).

**Table 3.** Direct Inactivation of HRV-2 and Inhibition of Viral Adsorption by Compound **2** and Pleconaril

| | plaque reduction (%) | |
|---|---|---|
| sample | direct inactivation of HRV-2 | inhibition of viral adsorption |
| pleconaril (0.25 µg/m) | 84.3[a] | 100.0; 93.1 |
| compound **2** (2.50 µg/mL) | not active | 35.2; 29.3 |

[a] Only one test.

**Serotype Alignment.** Although the 3D structure of HRV-16 was used as the starting point for pharmacophore model generation, the virtual hits **2** and **3** showed a distinct antiviral selectivity against HRV-2. We tried to rationalize this via detailed comparison of the hydrophobic canyons of HRV-16 and HRV-2, including their pocket factors.[36,52] First of all, the overall similarity was explored by a comparison of the amino acid sequences of HRV-2 and HRV-16 VP1 subunits using BLAST 2.2.17.[53] All amino acid residues involved in ligand binding showed 100% match in both HRV subtypes (Supporting Information Table S3). Additionally, the amino acid residues lining the binding pockets of the hydrophobic canyons were overlaid using LigandScout (Figure 6).[50] The overall very low rmsd of 0.433 Å confirmed the high similarity of the binding pockets.

The mechanism of action of HRV coat protein binders involves only a small conformational change of the viral coat depending on the ligand bound in the hydrophobic canyon. Inhibitors that reach into the toe of the canyon make the binding pocket less flexible and induce minor conformational changes in the overall protein structure.[19] Although the hydrophobic canyons of HRV-2 and HRV-16 have nearly identical conformations when bound to their natural pocket factors, binding of ligands may lead to different conformational changes in the viral coat proteins in both subtypes. Unfortunately, there are no X-ray crystal structures published that show HRV-2 and HRV-16 complexed with the same inhibitor, so no direct investigation and conformation comparison is possible. Generally, reasons for different inhibitor-induced conformational changes can lie in structural dissimilarities in neighboring parts of the protein, for example the second shell of amino acid residues lining the ligand binding pocket. This may explain why a compound may have different effects on HRV-2 and HRV-16 replication cycle progression. For example, pleconaril shows over 10-fold more potent inhibition of HRV-2 ($EC_{50} = 0.04$ µM) vs HRV-16 ($EC_{50} = 0.57$ µM).[8] Additionally, chemical features of pharmacophore models imply a certain degree of geometrical variance defined by the tolerance sphere located on the feature point. Usually, this tolerance is around 1.0−1.5 Å. It is therefore obvious that very small conformational differences in the binding site of modeled proteins (as is the case here for HRV-2 and HRV-16) cannot be reflected by a pharmacophore model. Thus, it is not surprising that inhibitors of related HRV subtypes are also identified by our model. Other possible explanations for different selectivity profiles include off-target effects, which may prevent the ligand from binding to the hydrophobic pocket in the first place. These effects are difficult to predict and not foreseeable by pharmacophore modeling or docking.

## Conclusions

Herbs and other naturally derived remedies described in ethnopharmacological sources mostly consist in simply prepared natural items whose chemical composition is complex. Many of the contained secondary metabolites, possibly active principles, have never been examined chemically or biochemically by using modern medical knowledge. They are however components of plant medicines that have stood the test of time and as such may offer clues of great interest to medicinal chemists. The strategy applied in this study uses molecular modeling data mining tools for a rational theoretical access to potential bioactive constituents of traditionally used remedies. This is exemplified in the search for natural products acting as inhibitors of the HRV coat protein. The antiviral activity of asafetida and its active constituents, farnesiferol C (**2**) and B (**3**), was discovered following the predictions of the pharmacophore-based virtual screening of a multiconformational 3D database (DIOS) consisting of almost 10 000 secondary metabolites from medicinal plants described some 2000 years ago. Compounds **2** and **3** represent novel chemical scaffolds with HRV-2 inhibiting potential in the low micromolar range. Though an application of the gum resin asafetida for the treatment of upper respiratory diseases has clearly been witnessed in Dioscorides' *De materia medica*, current uses mainly focus on its properties as a spice and a digestive supplement. The obtained data however underline the ancient pharmacological profile of asafetida. This study exemplarily confirms the applicability and potency of the combined theoretical (in silico) and empirical (ethnopharmacological) efforts for the rational search for naturally derived drug leads, enabling a fast and efficient identification of potential new inhibitors of the HRV-2 coat protein.

## Experimental Section

**Molecular Modeling.** All molecular modeling studies were performed using Catalyst 4.11 (Accelrys Inc., Catalyst version 4.11,

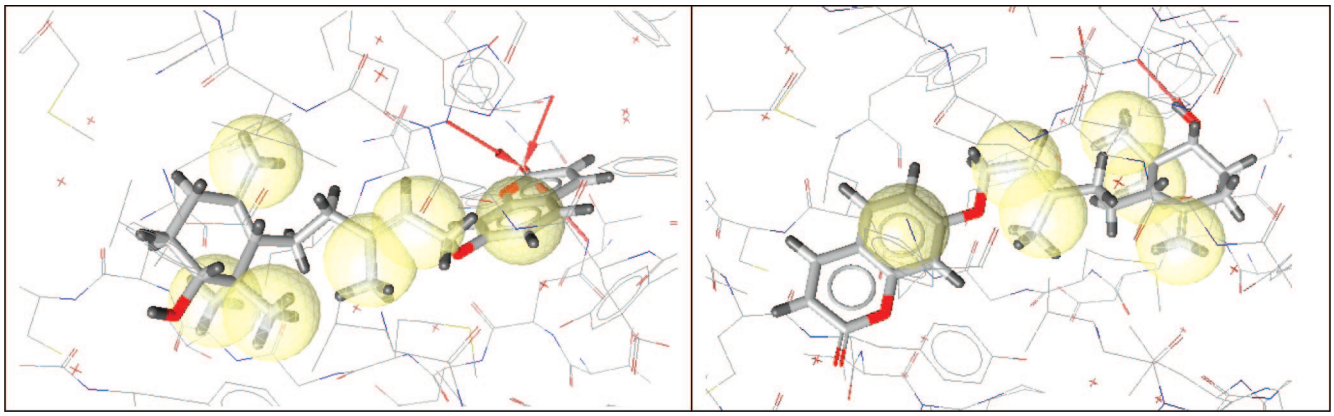

**Figure 4.** Two poses of compound **3** docked into the hydrophobic pocket of the HRV coat protein (automatic pharmacophore recognition using the software LigandScout). Pharmacophore features are color-coded: HBA (red) and H (yellow). Hydrogen bonds recognized to Leu100, Gln101, and Asn212 (left image) and to Leu100 (right image).

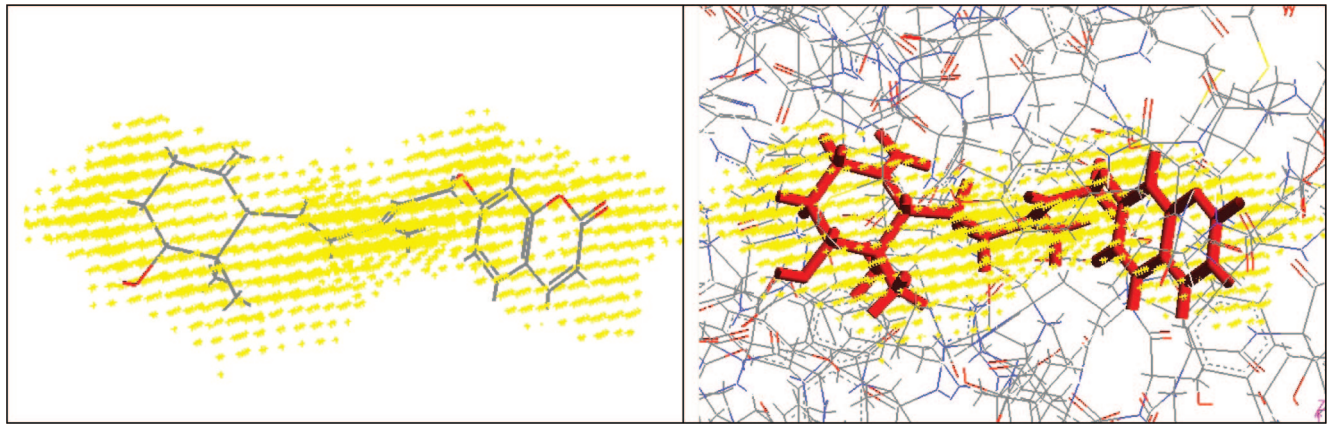

**Figure 5.** Compound **3** docked into the binding site (yellow) in LigandFit module in Cerius$^2$.

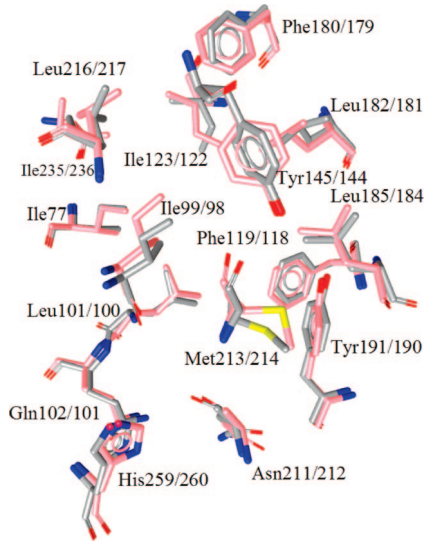


**Figure 6.** Overlay of the canyon amino acid residues of HRV-2 (gray, PDB entry 1V9U) and HRV-16 (rose, PDB entry 1AYM). Amino acid residues are indicated for HRV-2/HRV-16, respectively.

San Diego, CA) and Cerius$^2$ (Accelrys Inc., Cerius$^2$ version 4.10, San Diego, CA) installed on a Silicon Graphics Octane desktop workstation equipped with a 300 MHz MIPS R12000 processor (512 MB RAM) running the Irix 6.5 operating system.

**DIOS 3D Database Generation.** We have previously built a searchable 3D database, called DIOS, which contains 9676 individual small-molecule weight natural compounds based on entries in the ethnopharmacological source *De materia medica*, witnessed by Pedanius Dioscorides (1st cent. AD). This treatise is written in five books and deals with approximately 1000 simple drugs (thereof about 800 plants), which were used in medical practice until modern times.[38,54,55] The first book deals with spices, oils, and trees, whereas the second book mainly describes animal products (milk, honey, etc.). Books three and four deal with herbs and roots, and book five describes different sorts of wines and minerals. Due to our priority of investigating plant constituents, we employed books one, three, and four for the ethnobotanical source, using Julius Berendes' edition from 1902[55] and Max Aufmesser's edition from 2002.[54] In case of doubt, we considered more proposals of plant species and followed the comments and recommendations of J. Berendes and his co-worker, the physician and botanist C. Fraas.[55] At present, two online databases of chemicals including NPs are available to us and were used to search for literature dealing with the isolation of secondary metabolites corresponding to the mentioned plant species: SciFinder Scholar[56] and Beilstein Crossfire.[57] Structural information about plant constituents, limited to a molecular weight between 150 and 700 Da, was then retrieved from the original literature. This revealed a variable number of structures associated with each plant.

Three-dimensional models of the NPs were built by using the structure editor within the Catalyst Software Package (Catalyst Version 4.7 Accelrys, San Diego, CA). Compounds were minimized by using the default parameters of the CHARMM force field in order to reduce internal strain energy. Multiconformational models were generated by randomized conformational analysis using the Poling algorithm[58,59] and stored in a binary database using the CatDB procedure within Catalyst (FAST algorithm for conformer generation, maximum number of conformers = 100).[24]

**Virtual Screening (VS).** VS experiments were conducted within Catalyst with the elaborated model as search queries applying the Best Flexible Search option. Compounds present in the DIOS database were stored as three-dimensional structure models in multiconformational data format, and an index was built according to the presence or absence of chemical features in the molecules. In the VS procedure, the index was searched for compounds fulfilling the requirements defined by the query pharmacophore. All molecules remaining were then fitted in each of their stored conformations by rigid rotation and translation in order to determine if the chemical features of the structures were able to map the requested functions of the pharmacophore model. In this step, a slight conformational change of the molecular structure is allowed for compounds that exhibit a "near miss" of the pharmacophore model (best flexible search algorithm). A compound is considered to be a hit only if all functions of the pharmacophore model are mapped by defined functions of the respective molecule. The quality of the fit (fitting value) depends on two parameters: the weights assigned to the hypothesis features and how close the features in the molecule are to the centers of the corresponding location constraints in the pharmacophore hypothesis. In the present study, weights were set to a value of one for all features.

Docking studies were carried out within the LigandFit module implemented in the Cerius$^2$ software package by using the cff force field (Cerius$^2$ version 4.10).[60] The 3D protein structure was represented by PDB entry 1C8M. Binding site definition resulted from the bound ligand pleconaril, and the investigated minimized hit structures were docked flexibly. Protein preparation and parameter setting were performed as in previous studies. For more detailed information, see refs 23 and 61. The default LigandFit interaction filter preferences remained unchanged except for the activation of "Allow HB to terminal O" and the deactivation of the thereby unnecessary settings "Acceptor include aromatic F" and "Metal acceptor include S". When using LigandFit interaction filters, the docking procedure is performed first, unaffected by the defined interactions. Only in a second step, the hit poses are inspected and ranked by their ability to satisfy those interaction patterns. We set a minimum feature requirement of three mapped interactions for a molecule to be kept.

**General Experimental Procedures.** Optical rotation was measured on a Perkin-Elmer 341 polarimeter at 25 °C in $CHCl_3$. NMR spectra of compounds **1**−**4** were recorded on a Bruker-DRX300 and Bruker-DRX600 at 300 K in $CDCl_3$ and calibrated to the residual nondeuterated solvent signals. Tables with NMR data of **1** and **4** are given in the Supporting Information. Upon request, NMR spectra can be obtained from the corresponding author. Identification of sesquiterpene coumarins in the crude extract was accomplished by HPLC-DAD-MS (Hewlett-Packard HP-1100 liquid chromatograph equipped with a DAD-detector) coupled with an Esquire 3000plus ion trap mass spectrometer (Bruker Daltonics) equipped with electrospray ionization (ESI) in positive and negative mode: spray voltage, 4.0 kV; the sheath gas, $N_2$, 30 psi and the dry gas, $N_2$, 6 l min $^{-1}$, 325 °C; scanning range, 50–1000 *m/z*. Column chromatography was performed under TLC monitoring using silica gel flash CC (silica gel 60, 40–63 $\mu$m, Merck) and Sephadex LH-20 (20–100 $\mu$m, Pharmacia). TLC was performed on silica gel 60 $F_{254}$ plates (0.25 mm, Merck) using n-hexane/ethyl acetate (3:2) as mobile phase; detection was performed with methanolic vanillin−sulfuric acid reagent. HPLC data were obtained on a Hewlett-Packard-HP-1100 system, equipped with a photodiode array detector and an autosampler. The LC was fitted with a Zorbax SB C-18 column (150 mm × 4.6 mm i.d., 3.5 $\mu$m particle size, Agilent) at a column temperature of 25 °C, a flow rate of 1.0 mL/min, and with an injection volume of 10 $\mu$L; UV detection wavelengths were set to 205 and 325 nm. The mobile phases consisted of A: water (bidest.) and B: acetonitrile; linear gradient: 0 min at 20% B; 15 min at 60% B; 35 min at 67% B; and 50 min at 98% B. All chemicals were analytical grade. Solvents were either analytical grade or puriss. grade and distilled before use.

**Plant Material.** Asafetida (DAB 6 quality) was purchased from Mag. Kottas, Heilkräuter (Vienna, Austria, control number: KLA-40217). A voucher specimen has been deposited in the Herbarium of the Department of Pharmacognosy, Institute of Pharmacy, University of Innsbruck, Austria.

**Extraction and Isolation.** Crushed asafetida (307 g) was defatted with petrol ether. The dichloromethane (DCM)-soluble part (204 g) of the remaining material was subjected to liquid/liquid partition to gain a petrol ether fraction (71.5 g), a methanol/water (1:1) fraction (1.9 g), and a DCM fraction (94.9 g). 15.1 g of the former extract was separated using Sephadex CC (4 cm × 95 cm) with DCM/acetone (85:15) as eluent to gain 11 fractions (A1−A11). A3 (2.03 g) was further fractionated using Sephadex CC (2 cm × 75 cm) with acetone as eluent to gain six fractions (B1−B6). B3 (1.69 g) was subjected to silica gel CC (2.5 cm × 45 cm) using a step gradient of n-hexane to ethyl acetate and from ethyl acetate stepwise to methanol to give 11 subfractions (C1−C11). Subfractions C7 (210 mg) and C9 (245 mg) were each precipitated from methanol to afford pure compound **2** (142 mg) and **3** (148 mg), respectively. Physical and spectroscopic data of both isolates agreed with those reported for farnesiferol C (**2**) and farnesiferol B (**3**).[40,41] Subfraction C8 (78 mg) was rechromatographed by Sephadex CC (2 cm × 85 cm) and eluted with methanol to afford four subfractions (D1−D4). D1 (27.8 mg) was obtained as a whitish microcrystalline powder (**1**): optical rotation $[\alpha]_D^{20}$ +35.9° ($CHCl_3$, *c* 1.9) and identified by mass spectrometry (pos. mode: *m/z* 382.7 $[M + H]^+$; 364.7 $[M + 1 - H_2O]^+$; neg. mode: *m/z* 399.4 $[M-H + H_2O]^-$) and NMR experiments (see Supporting Information) as microlobidene.[39] Subfraction C11 (470 mg) was as well rechromatographed by Sephadex CC (2 cm × 85 cm) and eluted with methanol to afford two subfractions (E1 and E2). E1 (181 mg) was obtained as a pale yellow, amorphous solid (**4**): optical rotation $[\alpha]_D^{20}$ +36.6° ($CHCl_3$, *c* 3.5). Identification was achieved by mass spectrometry (pos. mode: *m/z* 441.7 $[M + H]^+$) and extensive 1D- and 2D-NMR experiments (see Supporting Information) and assigned to kellerin by comparison with literature.[42] Compounds **1**−**4** showed HPLC and $^1$H NMR purities of >95% with spectroscopic and spectrometric parameters (UV, MS, NMR) identical with the literature.

**Biological Testing. Evaluation of Cytotoxicity.** To determine the 50% cytotoxic concentration ($CC_{50}$), two-day-old confluent HeLa cell monolayer grown in 96-well plates was incubated with serial 2-fold dilutions of compounds for 72 h (37 °C, 5% $CO_2$). Then, the cells were fixed and stained with a crystal violet formalin solution as described previously.[62] After dye extraction, the optical density of individual wells was quantified spectrophotometrically at 550/630 nm with a microplate reader. Cell viability of individual compound-treated wells was evaluated as the percentage of the mean value of optical density resulting from six mock-treated cell controls, which was set at 100%. The 50% cytotoxic concentration ($CC_{50}$) was defined as the compound concentration reducing the viability of untreated cell cultures by 50%.

**Inhibition of Cytopathic Effect.** CPE inhibitory assays have been performed as described previously in one-day-old confluent HeLa cell monolayers growing in 96-well flat-bottomed microtiter plates (Falcon 3075).[45] After removal of culture medium, 50 $\mu$L of drug solution and a constant amount of virus in a volume of 50 $\mu$L (multiplicity of infection of 0.005 of HRV-1A and -16, 0.01 of HRV-2, and 0.15 of HRV-14) were added to the cells. Six wells of uninfected and six wells of infected cells without the test compound served as cell and virus control, respectively, on each plate. Pleconaril was used as a reference compound. By using the crystal violet uptake assay described for cytotoxic investigations, the inhibition of the virus-induced CPE was scored 72 h after infection when untreated infected control cells showed maximum cytopathic effect and the pleconaril-treated wells a 50% protection at a concentration of 0.01 (HRV-2) or 0.02 $\mu$g/mL (HRV-1A, -14, and -16).

**Modified Plaque Reduction Assays.** To investigate direct virus inactivation, approximately $10^6$ pfu of HRV-2 was incubated with 2.5 $\mu$g/mL of compound **2**, 0.25 $\mu$g/mL of pleconaril, and without the inhibitors in test medium at 37 °C for 60 min. Then, the virus suspensions were diluted 1:100, resulting in noneffective inhibitor concentrations. The residual virus titer was determined by plaque

assay. Briefly, medium was aspirated from 2-day-old HeLa cells grown in 12-well plates, and the cells were infected with 1 mL of the virus suspension. The plates were incubated for 1 h at 37 °C in 5% $CO_2$, after which the inoculum was replaced with overlay medium containing 0.4% agar without inhibitor.

To compare the effect on virus adsorption, 2.5 $\mu$g/mL of compound **2** and 0.25 $\mu$g/mL of pleconaril were added to 2-day-old HeLa cells grown in 12-well plates. Then, cell monolayer was infected with 50–100 pfu of HRV-2. Virus adsorption was performed at 4 °C for 2 h. Afterward, free virus and inhibitor were removed, and the cells were overlaid with medium containing 0.4% agar without inhibitor.

Each inhibitor was tested in triplicate. At least three untreated virus controls and one uninfected untreated cell control were included in all assays. The cell cultures were incubated until plaques appeared (3 days) and then fixed and stained with a solution of 0.4% crystal violet in a mixture of formalin (3% v/v) and ethanol (1.67% v/v) in water overnight. Plaques were counted over a light box after removal of the agar overlay. Two tests were performed.

**Acknowledgment.** This work was supported by a grant from the "Nachwuchsförderung" of the Leopold-Franzens University of Innsbruck awarded to J.M.R. The authors thank Inte:Ligand for providing the LigandScout software free of charge and Dr. S. Sturm for LC-MS measurements.

**Supporting Information Available:** Tables with NMR spectral data of compounds **1** and **4**, chemical structures of **1** and **4** with 1D-NOESY results for configurational assignment, and sequence alignment of VP1 of the HRV serotypes 2 and 16. This material is available free of charge via the Internet at http://pubs.acs.org.

## References

(1) Uncapher, C. R.; Dewitt, C. M.; Colonno, R. J. The major and minor group receptor families contain all but one human rhinovirus serotype. *Virology* **1991**, *180*, 814–817.
(2) Arruda, E.; Pitkaranta, A.; Witek, T. J., Jr.; Doyle, C. A.; Hayden, F. G. Frequency and natural history of rhinovirus infections in adults during autumn. *J. Clin. Microbiol.* **1997**, *35*, 2864–2868.
(3) Patick, A. K. Rhinovirus chemotherapy. *Antiviral Res.* **2006**, *71*, 391–396.
(4) Anzueto, A.; Niederman, M. S. Diagnosis and treatment of rhinovirus respiratory infections. *Chest* **2003**, *123*, 1664–1672.
(5) Michelow, I. C.; Olsen, K.; Lozano, J.; Rollins, N. K.; Duffy, L. B.; Ziegler, T.; Kauppila, J.; Leinonen, M.; McCracken, G. H., Jr. Epidemiology and clinical characteristics of community-acquired pneumonia in hospitalized children. *Pediatrics* **2004**, *113*, 701–707.
(6) Miller, E. K.; Lu, X.; Erdman, D. D.; Poehling, K. A.; Zhu, Y.; Griffin, M. R.; Hartert, T. V.; Anderson, L. J.; Weinberg, G. A.; Hall, C. B.; Iwane, M. K.; Edwards, K. M. Rhinovirus-associated hospitalizations in young children. *J. Infect. Dis.* **2007**, *195*, 773–781.
(7) Shih, S.-R.; Chen, S.-J.; Hakimelahi, G. H.; Liu, H.-J.; Tseng, C.-T.; Shia, K.-S. Selective human enterovirus and rhinovirus inhibitors: an overview of capsid-binding and protease-inhibiting molecules. *Med. Res. Rev.* **2004**, *24*, 449–474.
(8) Ledford, R. M.; Patel, N. R.; Demenczuk, T. M.; Watanyar, A.; Herbertz, T.; Collett, M. S.; Pevear, D. C. VP1 sequencing of all human rhinovirus serotypes: insights into genus phylogeny and susceptibility to antiviral capsid-binding compounds. *J. Virol.* **2004**, *78*, 3663–3674.
(9) Pevear, D. C.; Tull, T. M.; Seipel, M. E.; Groarke, J. M. Activity of pleconaril against enteroviruses. *Antimicrob. Agents Chemother.* **1999**, *43*, 2109–2115.
(10) Schmidtke, M.; Hammerschmidt, E.; Schueler, S.; Zell, R.; Birch-Hirschfeld, E.; Makarov, V. A.; Riabova, O. B.; Wutzler, P. Susceptibility of coxsackievirus B3 laboratory strains and clinical isolates to the capsid function inhibitor pleconaril: antiviral studies with virus chimeras demonstrate the crucial role of amino acid 1092 in treatment. *J. Antimicrob. Chemother.* **2005**, *56*, 648–656.
(11) Fleischer, R.; Laessig, K. Safety and efficacy evaluation of pleconaril for treatment of the common cold. *Clin. Infect. Dis.* **2003**, *37*, 1722.
(12) Hayden, F. G.; Herrington, D. T.; Coats, T. L.; Kim, K.; Cooper, E. C.; Villano, S. A.; Liu, S.; Hudson, S.; Pevear, D. C.; Collett, M.; McKinlay, M. Efficacy and safety of oral pleconaril for treatment of colds due to picornaviruses in adults: results of 2 double-blind, randomized, placebo-controlled trials. *Clin. Infect. Dis.* **2003**, *36*, 1523–1532.
(13) Pevear, D. C.; Hayden, F. G.; Demenczuk, T. M.; Barone, L. R.; McKinlay, M. A.; Collett, M. S. Relationship of pleconaril susceptibility and clinical outcomes in treatment of common colds caused by rhinoviruses. *Antimicrob. Agents Chemother.* **2005**, *49*, 4492–4499.
(14) Greve, J. M.; Davis, G.; Meyer, A. M.; Forte, C. P.; Connolly Yost, S.; Marlor, C. W.; Kamarck, M. E.; McClelland, A. The major human rhinovirus receptor is ICAM-1. *Cell* **1989**, *56*, 839–47.
(15) Staunton, D. E.; Merluzzi, V. J.; Rothlein, R.; Barton, R.; Marlin, S. D.; Springer, T. A. A cell adhesion molecule, ICAM-1, is the major surface receptor for rhinoviruses. *Cell* **1989**, *56*, 849–53.
(16) Andries, K.; Dewindt, B.; Snoeks, J.; Willebrords, R.; Stokbroekx, R.; Lewi, P. J. A comparative test of fifteen compounds against all known human rhinovirus serotypes as a basis for a more rational screening program. *Antiviral Res.* **1991**, *16*, 213–25.
(17) Rossmann, M. G. The structure of antiviral agents that inhibit uncoating when complexed with viral capsids. *Antiviral Res.* **1989**, *11*, 3–13.
(18) Rossmann, M. G. The canyon hypothesis. *Viral Immunol.* **1989**, *2*, 143–161.
(19) Hadfield, A. T.; Diana, G. D.; Rossmann, M. G. Analysis of three structurally related antiviral compounds in complex with human rhinovirus 16. *Proc. Natl. Acad. Sci. U.S.A.* **1999**, *96*, 14730–14735.
(20) Kolatkar, P. R.; Bella, J.; Olson, N. H.; Bator, C. M.; Baker, T. S. Structural studies of two rhinovirus serotypes complexed with fragments of their cellular receptor. *EMBO J.* **1999**, *18*, 6249–6259.
(21) Langer, T.; Hoffmann, R. D. Pharmacophore modelling: applications in drug discovery. *Expert Opin. Drug Discovery* **2006**, *1*, 261–267.
(22) Rollinger, J. M.; Langer, T.; Stuppner, H. Strategies for efficient lead structure discovery from natural products. *Curr. Med. Chem.* **2006**, *13*, 1491–1507.
(23) Steindl, T.; Langer, T.; Crump, C. E.; Hayden, F. G. Pharmacophore modeling, docking, and principal component analysis-based clustering: combined computer-assisted approaches to identify new inhibitors of the human rhinovirus coat protein. *J. Med. Chem.* **2005**, *48*, 6250–6260.
(24) Rollinger, J. M.; Haupt, S.; Stuppner, H.; Langer, T. Combining ethnopharmacology and virtual screening for lead structure discovery: COX-inhibitors as application example. *J. Chem. Inf. Comput. Sci.* **2004**, *44*, 480–488.
(25) Samimi, M. N.; Unger, W. The gum resins of Afghan asafetida-producing ferula species. Source and quality of Afghan asafetida. *Planta Med.* **1979**, *36*, 128–33.
(26) Kubetzka, K.; Bohn, I. In *Hagers Handbuch der Pharmazeutischen Praxis, Folgeband 2*; Blaschek, W., Hänsel, R., Keller, K., Reichling, J., Rimpler, H., Schneider, G., Eds.; Springer: Berlin, Germany, 1998; pp 696–713.
(27) Appendino, G.; Tagliapietra, S.; Nano, G. M.; Jakupovic, J. Sesquiterpene coumarin ethers from Asafetida. *Phytochemistry* **1994**, *35*, 183–186.
(28) Abd El-Razek, M. H.; Ohta, S.; Hirata, T. Terpenoid coumarins of the genus Ferula. *Heterocycles* **2003**, *60*, 689–716.
(29) Iranshahi, M.; Arfa, P.; Ramezani, M.; Jaafari, M. R.; Sadeghian, H.; Bassarello, C.; Piacente, S.; Pizza, C. Sesquiterpene coumarins from Ferula szowitsiana and in vitro antileishmanial activity of 7-prenyloxycoumarins against promastigotes. *Phytochemistry* **2007**, *68*, 554–561.
(30) Appendino, G.; Maxia, L.; Bascope, M.; Houghton, P. J.; Sanchez-Duffhues, G.; Munoz, E.; Sterner, O. A meroterpenoid NF-$\kappa$ B inhibitor and drimane sesquiterpenoids from asafetida. *J. Nat. Prod.* **2006**, *69*, 1101–1104.
(31) Lahouel, M.; Zini, R.; Zellagui, A.; Rhouati, S.; Carrupt, P.-A.; Morin, D. Ferulenol specifically inhibits succinate ubiquinone reductase at the level of the ubiquinone cycle. *Biochem. Biophys. Res. Commun.* **2007**, *355*, 252–257.
(32) Motai, T.; Daikonya, A.; Kitanaka, S. Sesquiterpene coumarins from *Ferula fukanensis* and nitric oxide production inhibitory effects. *J. Nat. Prod.* **2004**, *67*, 432–436.
(33) Rollinger, J. M.; Hornick, A.; Langer, T.; Stuppner, H.; Prast, H. Acetylcholinesterase inhibitory activity of scopolin and scopoletin discovered by virtual screening of natural products. *J. Med. Chem.* **2004**, *47*, 6248–6254.
(34) Rollinger, J. M.; Bodensieck, A.; Seger, C.; Ellmerer, E. P.; Bauer, R.; Langer, T.; Stuppner, H. Discovering COX-inhibiting constituents of *Morus* root bark: activity-guided versus computer-aided methods. *Planta Med.* **2005**, *71*, 399–405.
(35) Berman, H. M.; Westbrook, J.; Feng, Z.; Gililand, G.; Bhat, T. N. The protein data bank. *Nucleic Acids Res.* **2000**, *28*, 235–242.
(36) Verdaguer, N.; Blaas, D.; Fita, I. Structure of human rhinovirus serotype 2 (HRV2). *J. Mol. Biol.* **2000**, *300*, 1179–1194.
(37) Lipinski, C. A.; Lombardo, F.; Dominy, B. W.; Feeney, P. J. Experimental and computational approaches to estimate solubility and permeability in drug discovery and development settings. *Adv. Drug Delivery Rev.* **1997**, *23*, 3–25.

(38) Beck, L. Y. (transl) *Pedanius Dioscorides of Anazarbus—De materia medica*; Olms-Weidmann: Hildesheim, Zürich, New York, 2005; pp 217–220.
(39) Nabiev, A. A.; Malikov, V. M. Microlobidene—a terpenoid coumarin from *Ferula microloba* with a novel terpenoid skeleton. *Khim. Prir. Soedin.* **1983**, *6*, 781–782.
(40) Caglioti, L.; Naef, H.; Arigoni, D.; Jeger, O. Zur Kenntnis der Sesquiterpene und Azulene: Über die Inhaltsstoffe der Asa foetida L. Farnesiferol A. *Helv. Chim. Acta.* **1958**, *42*, 2278–2292.
(41) Nassar, M. I.; Abu-Mustafa, E. A.; Ahmed, A. A. Sesquiterpene coumarins from *Ferula assafoetida* L. *Pharmazie* **1995**, *50*, 766–767.
(42) Perel'son, M. E.; Sheichenko, V. I.; Sklyar Yu, E.; Andrianova, V. B. Configuration of kellerin and samarkandin. *Khim. Farm. Zh.* **1977**, *11*, 33–36.
(43) Andrianova, V. B.; Sklyar, Yu. E.; Perel'son, M. E.; Pimenov, M. G. Kellerin, a new coumarin from *Ferula kelleri* roots. *Khim. Prir. Soedin.* **1973**, *6*, 795–796.
(44) (a) Nabiev, A. A.; Khasanov, T. K.; Malikov, V. M. *Khim. Prir. Soedin.* **1982**, *5*, 578–581. (b) Nabiev, A. A.; Khasanov, T. K.; Malikov, V. M. *Chem. Nat. Compd.* **1982**, *18*, 547–549, English translation of ref 44a.
(45) Makarov, V. A.; Riabova, O. B.; Granik, V. G.; Wutzler, P.; Schmidtke, M. Novel [(biphenyloxy)propyl]isoxazole derivatives for inhibition of human rhinovirus 2 and coxsackievirus B3 replication. *J. Antimicrob. Chemother.* **2005**, *55*, 483–488.
(46) Andries, K.; Dewindt, B.; Snoeks, J.; Wouters, L.; Moereels, H.; Lewi, P. J.; Janssen, P. A. J. Two groups of rhinoviruses revealed by a panel of antiviral compounds present sequence divergence and differential pathogenicity. *J. Virol.* **1990**, *64*, 1117–23.
(47) Ninomiya, Y.; Aoyama, M.; Umeda, I.; Suhara, Y.; Ishitsuka, H. Comparative studies on the modes of action of the antirhinovirus agents Ro 09-0410, Ro 09-0179, RMI-15,731, 4′,6-dichloroflavan, and enviroxime. *Antimicrob. Agents Chemother.* **1985**, *27*, 595–599.
(48) Pevear, D. C.; Fancher, M. J.; Felock, P. J.; Rossmann, M. G.; Miller, M. S.; Diana, G.; Treasurywala, A. M.; McKinlay, M. A.; Dutko, F. J. Conformational change in the floor of the human rhinovirus canyon blocks adsorption to HeLa cell receptors. *J. Virol.* **1989**, *63*, 2002–2007.
(49) Dewindt, B.; van Eemeren, K.; Andries, K. Antiviral capsid-binding compounds can inhibit the adsorption of minor receptor rhinoviruses. *Antiviral Res.* **1994**, *25*, 67–72.
(50) Wolber, G.; Langer, T. LigandScout: 3-D pharmacophores derived from protein-bound ligands and their use as virtual screening filters. *J. Chem. Inf. Comput. Sci.* **2005**, *45*, 160–169, available from Inte: Ligand GmbH, www.inteligand.com/ligandscout.
(51) Böhm, H. J.; Klebe, G.; Kubinyi, H. *Wirkstoffdesign*; Spektrum Akademischer Verlag GmbH: Berlin, Germany, 1996; Chapter *18*, pp 327–348.
(52) Hadfield, A. T.; Lee, W.; Zhao, R.; Oliveira, M. A.; Minor, I.; Rueckert, R. R.; Rossman, M. G. The refined structure of human rhinovirus 16 at 2.15 ANG resolution: implications for the viral life cycle. *Structure* **1997**, *5*, 427–441.
(53) Tatusova, T. A.; Madden, T. L. Blast 2 sequences, a new tool for comparing protein and nucleotide sequences. *FEMS Microbiol. Lett.* **1999**, *174*, 247–250.
(54) Aufmesser, M. Pedanius Dioscurides aus Anazarba—Fünf Bücher über die Heilkunde. In *Altertumswissenschaftliche Texte und Studien*; Olms-Weidmann Verlag: New York, 2002; Band *37*.
(55) Berendes, J. *Des Pedanios Dioskurides aus Anazarbos Arneimittellehre in fünf Bücher*; Stuttgart, 1902; reprint: Sändig Reprints Verlag: Vaduz, FL, 1997.
(56) SciFinder Scolar; American Chemical Society: http://www.cas.org/products/sfacad/.
(57) Beilstein Crossfire; MDL Information Systems: http://www.beilstein-.com/ (November 2007: http://www.mdl.com/products/knowledge/crossfire_beilstein/).
(58) Smellie, A.; Kahn, S. D.; Teig, S. L. Analysis of conformational coverage. 1. Validation and estimation of coverage. *J. Chem. Inf. Comput. Sci.* **1995**, *35*, 285–294.
(59) Smellie, A.; Teig, S. L.; Towbin, P. Poling: promoting conformational variation. *J. Comput. Chem.* **1995**, *16*, 171–187.
(60) Venkatachalam, C. M.; Jiang, X.; Oldfield, T.; Waldman, M. LigandFit: a novel method for the shape-directed rapid docking of ligands to protein active sites. *J. Mol. Graphics Modell.* **2003**, *21*, 289–307.
(61) Steindl, T.; Langer, T. Docking versus pharmacophore model generation: a comparison of high-throughput virtual screening strategies for the search of human rhinovirus coat protein inhibitors. *QSAR Comb. Sci.* **2005**, *24*, 470–479.
(62) Schmidtke, M.; Schnittler, U.; Jahn, B.; Dahse, H.-M.; Stelzner, A. A rapid assay for evaluation of antiviral activity against coxsackie virus B3, influenza virus A, and herpes simplex virus type 1. *J. Virol. Methods* **2001**, *95*, 133–143.

JM701494B